Environmental Science & Technology

pubs.acs.org/est

Article

Particle Resuspension Dynamics in the Infant Near-Floor Microenvironment

Tianren Wu, Manjie Fu, Maria Valkonen, Martin Täubel, Ying Xu, and Brandon E. Boor*

Cite This: *Environ. Sci. Technol.* 2021, 55, 1864–1875

Read Online

ACCESS | Metrics & More | Article Recommendations | Supporting Information

ABSTRACT: Carpet dust contains microbial and chemical material that can impact early childhood health. Infants may be exposed to greater quantities of resuspended dust, given their close proximity to floor surfaces. Chamber experiments with a robotic infant were integrated with a material balance model to provide new fundamental insights into the size-dependency of infant crawling-induced particle resuspension and exposure. The robotic infant was exposed to resuspended particle concentrations from 10^5 to 10^6 m^{-3} in the near-floor (NF) microzone during crawling, with concentrations generally decreasing following vacuum cleaning of the carpets. A pronounced vertical variation in particle concentrations was observed between the NF microzone and bulk air. Resuspension fractions for crawling are similar to those for adult walking, with values ranging from 10^{-6} to 10^{-1} and increasing with particle size. Meaningful amounts of dust are resuspended during crawling, with emission rates of 0.1 to 2 × 10^4 $\mu g\ h^{-1}$. Size-resolved inhalation intake fractions ranged from 5 to 8 × 10^3 inhaled particles per million resuspended particles, demonstrating that a significant fraction of resuspended particles can be inhaled. A new exposure metric, the dust-to-breathing zone transport efficiency, was introduced to characterize the overall probability of a settled particle being resuspended and delivered to the respiratory airways. Values ranged from less than 0.1 to over 200 inhaled particles per million settled particles, increased with particle size, and varied by over 2 orders of magnitude among 12 carpet types.

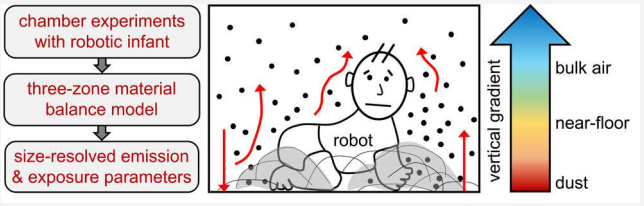

INTRODUCTION

We are perpetually surrounded by a cloud of self-induced resuspended particles, referred to as the "perihuman cloud effect."[1] As we walk across the carpet or move in bed, we continually stir-up settled indoor dust.[2−4] The process of settled particles detaching from a surface and becoming airborne through the application of aerodynamic, mechanical, and electrostatic removal forces is referred to as resuspension. Resuspension associated with human activities and disturbances of dust deposits can be a significant source of coarse mode particles (size (D_p): 1 to 10 μm) indoors and to a lesser extent submicron particles.[5,6] Emission rates of PM_{10} ($D_p \leq 10$ μm) for adult walking-induced resuspension are on the order of 1 to 10 mg min^{-1}, which is comparable to emissions from vacuuming, frying, smoking, and incense burning.[4]

Infants are very physically active indoors. As infants crawl, play, and learn to walk, we expect them to generate their own dust clouds. Crawling and walking infants from 12 to 19 months old can take 200 to 2500 steps h^{-1} indoors.[7−10] Walking and crawling infants have been found to be in motion 33 and 20% of the time, respectively, with walkers traveling three times the distance as crawlers.[11] With an average of 500 to 1500 walking steps h^{-1}, infants can take upwards of 9000 walking steps and travel the length of 20 football fields each day.[12] The moving paths of infants within a room are incredibly variable in terms of length, direction, speed, and shape as they decide when and where to move in an unpredictable manner. Video coded time-series data indicates that the locomotion of infants is highly transient, with constantly varying activity types, such as crawling, waving arms, being still, and playing, and locomotion often does not exhibit any obvious pattern.[13,14] The factors influencing infant locomotion include age, locomotion experience and type, and external factors such as the presence of obstacles, toys, or caretakers.[9,10]

Despite the extent of infant movement across dust-bearing indoor surfaces, we have a poor understanding of how infants and their activities induce the resuspension of settled particles. Infants are likely to be exposed to elevated concentrations of resuspended dust, given their close proximity to surfaces, such as carpet, hard flooring, and crib mattress bedding. Infant movement-induced resuspension may play an important, yet presently unknown, role in contributing to their inhalation exposures to the diverse spectrum of the biological and chemical content of house dust. Our recent work[15] demonstrated that infant crawling-induced resuspension is a

Received: September 12, 2020
Revised: December 14, 2020
Accepted: December 18, 2020
Published: January 15, 2021

https://dx.doi.org/10.1021/acs.est.0c06157
Environ. Sci. Technol. 2021, 55, 1864–1875

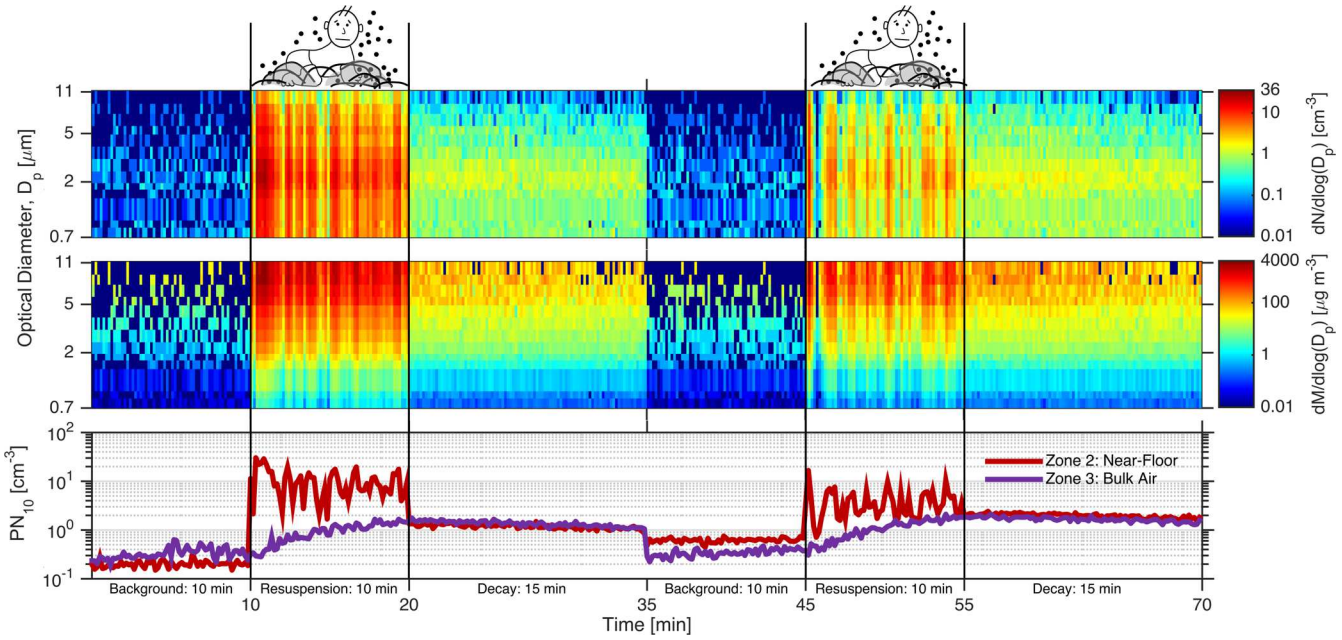

Figure 1. Particle number ($dN/d\log D_p$, cm^{-3}, top) and mass ($dM/d\log D_p$, $\mu g\ m^{-3}$, middle) size distribution time-series as measured in the infant NF microzone and size-integrated particle number concentration (PN_{10}, cm^{-3}, bottom) time-series as measured in the NF microzone (red) and BA zone (purple) during two resuspension sequences on carpet H.

major source of airborne biological particulate matter (bioPM), increasing inhalation exposure by 0.5 to 2 cm^{-3} in the infant breathing zone, with much of the bioPM depositing in the lower regions of the respiratory system.

Dust deposited on carpet surfaces, or embedded between carpet fibers, consists of a complex mixture of chemical and biological material. The biological content of carpet dust includes various living and dead microorganisms (e.g., bacteria, archaea) and other materials of biological origin, such as dispersal items (e.g., pollen grains) and biological excretions and debris (e.g., animal and mite allergens).[16−21] A variety of semivolatile organic compounds (SVOCs) can partition to settled dust (SD) particles, such as fluorinated soil retardants (e.g., PFAS),[22−24] antimicrobials (e.g., triclosan),[25] phthalate plasticizers,[26] organohalogen and organophosphorus flame retardants,[27] and polyaromatic hydrocarbons,[28] all of which are of concern for human health. Dust may also contain toxic metals, such as lead.[29−34] Carpets can serve as a reservoir of particles that can be delivered to an infant's breathing zone via resuspension. Exposure to certain chemical compounds and microbes has been associated with adverse health effects, including asthma, wheezing, respiratory infections, and several allergic symptoms.[35−45] On the other hand, early-life exposure to diverse and abundant bacteria and fungi, certain microbial excretions and components, and allergenic proteins of dust mites and animal dander has been linked to a reduced prevalence of asthma, atopy, wheezing, hay fever, and allergies later in life.[16,46−55] In addition, microbial cells in house dust can release volatile organic compounds (VOCs) because of their metabolism, which may induce allergic responses.[56−62]

Currently, there is limited knowledge on the transport of SD during crawling-induced resuspension events and infant exposure to self-induced resuspended dust. In this study, a new set of chamber experiments were conducted to mechanistically evaluate carpet dust resuspension initiated by infant crawling and to provide new fundamental insights into infant exposure to their "personal" particle cloud in their near-floor (NF) microzone. A three-zone material balance model was applied to characterize resuspension dynamics and to evaluate size-resolved resuspension parameters, including the resuspension fraction, resuspension rate, and emission rate. The effect of vacuuming on resuspended particle concentrations in the infant NF microzone was investigated to understand how it can reduce infant inhalation exposure to carpet dust. The inhalation intake fraction, which accounts for all factors that potentially affect the source-receptor inhalation pathway,[3,63−65] was estimated for infants to provide a mechanistic link between the emission source and infant exposure. More importantly, we introduce a new quantitative exposure metric, the dust-to-breathing zone transport efficiency, which we define as the overall likelihood of a settled particle on a surface to resuspend and be inhaled into the respiratory airways. This work will provide the aerosol physics and exposure science communities with source term inputs for improving material balance modeling of resuspension and understanding its role in shaping early-life exposures to the microbial, allergenic, and chemical content of indoor SD.

MATERIALS AND METHODS

Experimental Design. Resuspension experiments were conducted in an 81.4 m^3 room-sized chamber operating at an air exchange rate of 0.66 h^{-1} and supplied with HEPA-filtered air (Figures S2 and S3). The crawling locomotion was performed by a simplified robotic infant moving across the carpet. n = 12 carpets (A−L), borrowed from residents in the Helsinki metropolitan region of Finland, were examined in this study (Figure S1, Table S1). They are "area rug" style carpets, which are commonly used in Finland and do not contain carpet padding. For each carpet, n = 6 10 min resuspension experiments were conducted, with n = 3 replicate tests sampling in the infant NF microzone and n = 3 replicate tests sampling in the bulk air (BA) of the chamber. All carpets were then vacuumed in a single cleaning event to explore the impact

https://dx.doi.org/10.1021/acs.est.0c06157
Environ. Sci. Technol. 2021, 55, 1864−1875

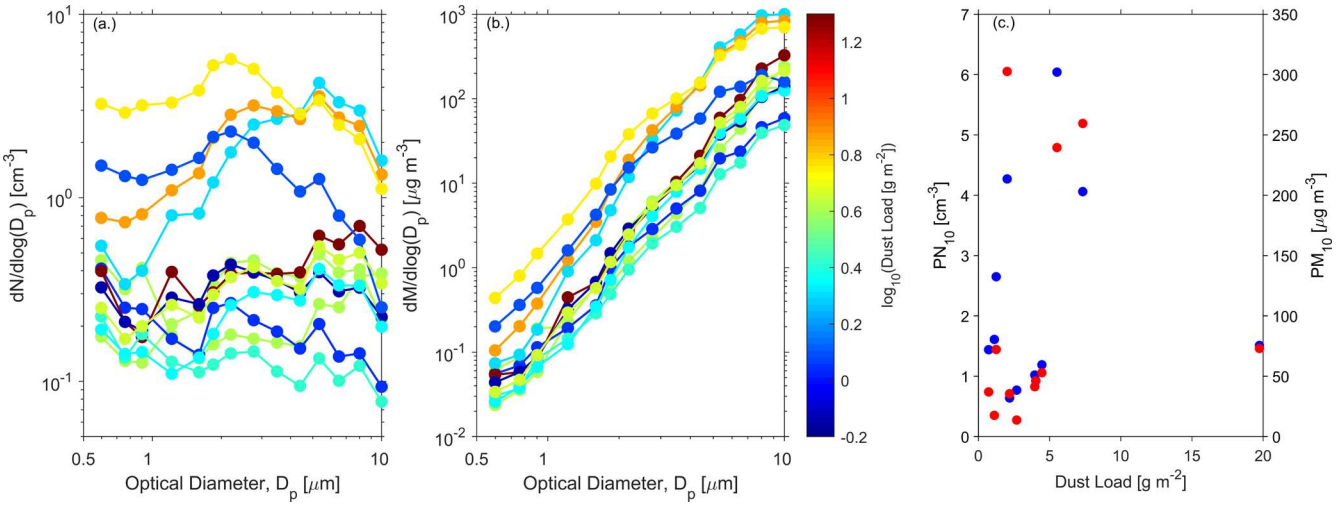

Figure 2. (a) Mean particle number ($dN/d\log D_p$, cm^{-3}) and (b) mass ($dM/d\log D_p$, $\mu g\ m^{-3}$) size distributions and (c) mean size-integrated particle number (PN_{10}, cm^{-3}) and mass (PM_{10}, $\mu g\ m^{-3}$) concentrations measured across all crawling paths for each carpet for the infant NF microzone. The color of the number and mass size distribution curves are defined by the $\log_{10}$(dust load, g m^{-2}) heat map. PN_{10} and PM_{10} are displayed as a function of the dust load (g m^{-2}), with blue markers corresponding to PN_{10} and red markers corresponding to PM_{10} Dust loads for each carpet can be found in Table S1, and size-integrated particle concentrations for both the NF and BA zones can be found in Tables S2 and S3.

of vacuuming on reducing infant exposure to resuspended particles. On the postvacuumed carpet, n = 3 replicate 10 min resuspension tests were conducted, sampling only in the infant NF microzone. In total, n = 108 10 min resuspension experiments were conducted (separate from those included in Wu et al.[15]). Each resuspension experiment includes a 10 min background period, a 10 min resuspension period, and a 15 min decay period.

An optical particle sizer (OPS, model 3330, TSI Inc.) was deployed to monitor the number size distribution ($dN/d\log D_p$, cm^{-3}) of the resuspended particles at the infant breathing zone height in the NF microzone or the BA for each resuspension experiment, with a measurement size range of D_p = 0.314 to 11.2 μm.[15] The SD from each carpet was collected at the end of the n = 6 NF and BA resuspension experiments and prior to vacuuming the carpets. The SD was used for gravimetric analysis and offline particle counting analysis (via PAMAS SVSS, Sensor: SLS-25/25, PAMAS GmbH) to determine the dust mass loading and settled particle number size distribution ($dL/d\log D_p$, m^{-2}). Additional details on the experimental setup and instrumentation are provided in the Supporting Information.

Three-Zone Material Balance Model. A three-zone material balance model (Figure S5), including the SD zone of the carpet, infant NF microzone, and BA zone, was employed to model the particle concentration in each zone and estimate the size-resolved resuspension and exposure parameters (eqs S1−S3). The three-zone material balance model is described in detail in the Supporting Information, along with the methodology for estimating size-resolved resuspension fractions (r_{aj}),[2,4−6,66−68] resuspension rates (RR_j, h^{-1}),[2,69−73] intake fractions (iF_j, ppm as inhaled particles per million resuspended particles), and dust-to-breathing zone transport efficiencies (Φ_j, ppm as inhaled particles per million settled particles). The three-zone model is a derivative of both the carpet-to-air two-zone model, which describes the transport process of SD between indoor surfaces and room air,[2,6,74] and the near-field/far-field model,[75−80] which accounts for imperfect air mixing and pollutant dispersion and improves human exposure assessment when the receptor is close to the emission source.

RESULTS AND DISCUSSION

Resuspension Sequence. The crawling motion of an infant can induce resuspension of SD, resulting in a significant elevation in particle concentrations in the infant NF microzone. This is illustrated in Figure 1, which shows the particle number (top) and mass (middle) size distribution time-series in the NF microzone and the size-integrated number concentrations (PN_{10}, bottom) in the NF (red) and BA (purple) before, during, and after a crawling event for two crawling paths on the same carpet. A significant increase in airborne particle concentrations in the infant NF microzone was observed immediately after the robot began crawling. The concentration remains elevated for the entirety of the crawling period. After cessation of crawling, the concentration decays rapidly in the NF microzone as the particles are removed via turbulent diffusion, which quickly transports the particles to the BA zone, and deposition by gravitational settling. In contrast, the BA particle concentration increases gradually during crawling periods and decreases slowly during decay periods. Concentrations in the NF microzone are up to 10 times higher than that in the BA during the crawling periods (Tables S2 and S3), indicating that the infant is surrounded by a high concentration of self-agitated resuspended particles during periods of active movement.

Particle Number/Mass Size Distributions and Size-Integrated Concentrations in the NF Zone. The mean number and mass size distributions of resuspended particles in the NF microzone exhibit more than 10-fold variation in magnitude across the 12 tested carpets (Figure 2a,b). The number size distributions do not present a consistent pattern in shape. In the submicron regime, some of them present a decreasing trend as part of another mode that is smaller than D_p = 0.5 μm, which was not captured by the OPS. A clear mode between D_p = 1.5 and 4 μm was observed on several carpets, which may be associated with bacterial cells and fungal spores according to our prior work.[15,20] The number size

https://dx.doi.org/10.1021/acs.est.0c06157
Environ. Sci. Technol. 2021, 55, 1864−1875

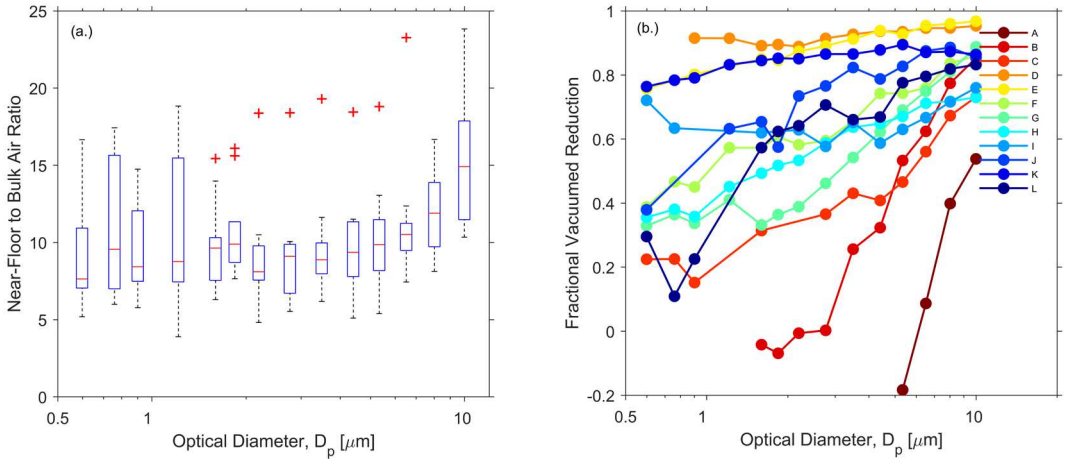

Figure 3. (a) Size-resolved ratios of the mean particle number concentrations in the infant NF microzone to the BA zone during crawling periods across all carpets. Box plots represent the interquartile range, whiskers represent the 5th and 95th percentiles, and markers represent outliers. Data for all carpets are compiled. (b) Size-resolved fractional vacuumed reductions for the 12 carpets (A–L). Note: to improve visualization of carpets B-L, values for D_p < 5 μm for carpet A are not shown.

distributions on some carpets show a mode between D_p = 5 and 9 μm. Previous indoor measurements based on laser-induced fluorescence techniques indicate that particles generated by occupants' movements with D_p > 6 μm mainly consist of biological content.[15,81,82] The mean mass size distribution for all carpets exhibits a monotonic increase with particle size.

The mean size-integrated mass concentrations (PM_{10}) for each carpet are also very different (Figures 2c and S7), with the majority ranging from 25 to 100 μg m^{-3} and for three carpets exceeding 200 μg m^{-3}. The mean size-integrated number concentrations (PN_{10}) varied from 0.6 to 6 cm^{-3}. The prominent variations in the concentrations and size distributions of resuspended particles among the 12 carpets are mainly attributed to differences in the size distribution of SD and the material and structure of carpets and their fibers.[2,4,6,66,83,84]

Relationship between Particle Number/Mass Size Distributions and Carpet Dust Mass Loads. Although prior resuspension chamber studies have found a positive correlation between the resuspended particle concentration and the dust mass loading of artificially seeded dust,[3,70,85] this feature was not observed in the current study. The color scheme of the number and mass size distributions in Figure 2a,b indicates the dust load of each carpet, which spans over a wide range from 0.72 to 19.74 g m^{-2} (Table S1). Figure 2c presents the mean size-integrated number and mass concentrations as a function of the dust load. Generally, the dust load does not exhibit an obvious correlation with the magnitude of the number and mass size distributions or the size-integrated concentrations of the resuspended particles in the crawling experiments. For example, carpet E has the highest dust load at 19.74 g m^{-2}, while it shows a moderate magnitude in number and mass size distributions among the 12 carpets (shown in dark red in Figure 2a,b). The mean size-integrated particle number and mass concentrations for carpet E are PN_{10} = 1.5 cm^{-3} and PM_{10} = 73 μg m^{-3}, which are only the fifth and fourth highest among all carpets, respectively.

Although settled floor dust is widely used as a surrogate in indoor inhalation exposure studies,[86−89] our results suggest that the dust load is not a good indicator for infants' exposure to resuspended particles in the NF microzone. The discrepancy between the dust load and the number and mass concentration of the resuspended particles reveals the complexity of the resuspension process from a carpet, which needs to account for factors other than the dust load, such as the uneven vertical distribution of settled particles,[90] particle physiochemical properties, and carpet material/structure. Artificial seeding processes for test dust may result in most particles embedded close to the carpet surface or in a relatively even distribution along the carpet fibers.[4,91] This may make the amount of resuspendable dust proportional to the dust load, and hence a positive correlation between the dust load and the resuspended particle concentration may be observed. However, in reality, the carpet dust loading process can result in an uneven vertical distribution of particles along the fibers. Thus, the fraction of dust available for resuspension may not present a clear correlation with the dust load.[90] Particle properties and carpet material/structure can affect adhesion forces between the particle and the carpet fiber surface, which further influence the resuspension process.[4,66,83,84]

Spatial Variations in Concentrations of Crawling-Induced Resuspended Particles. Resuspended particles exhibit a pronounced vertical variation in concentration during crawling periods. On average, the size-resolved particle number concentrations in the NF microzone are 6 to 10 times higher than in the BA for D_p < 8 μm and >10 times higher for D_p > 8 μm during crawling periods across all 12 carpets (Figure 3a). The ratio of the number concentration between the two zones increases with particle size from D_p = 3 to 11 μm, suggesting that the spatial variation generally becomes more pronounced with increasing particle size as the particle gravitational settling velocity and deposition rate increase (Figure S6).

The spatial variation in particle concentrations indicates that the infant is surrounded by a highly concentrated cloud of resuspended particles.[1,92,93] This personal cloud is formed because the particles are only released from the carpet in the area where there is contact between the robotic infant and the carpet or where the vibration of the carpet and wake generated by the robotic infant is strong enough to detach the SD, both of which are centered around the robotic infant. In addition, the mixing induced by the crawling locomotion is too weak to aid in uniform dispersion of particles in the chamber, thereby enhancing the personal cloud effect. A previous study indicates that intensive indoor movements, such as walking, result in a

https://dx.doi.org/10.1021/acs.est.0c06157
Environ. Sci. Technol. 2021, 55, 1864−1875

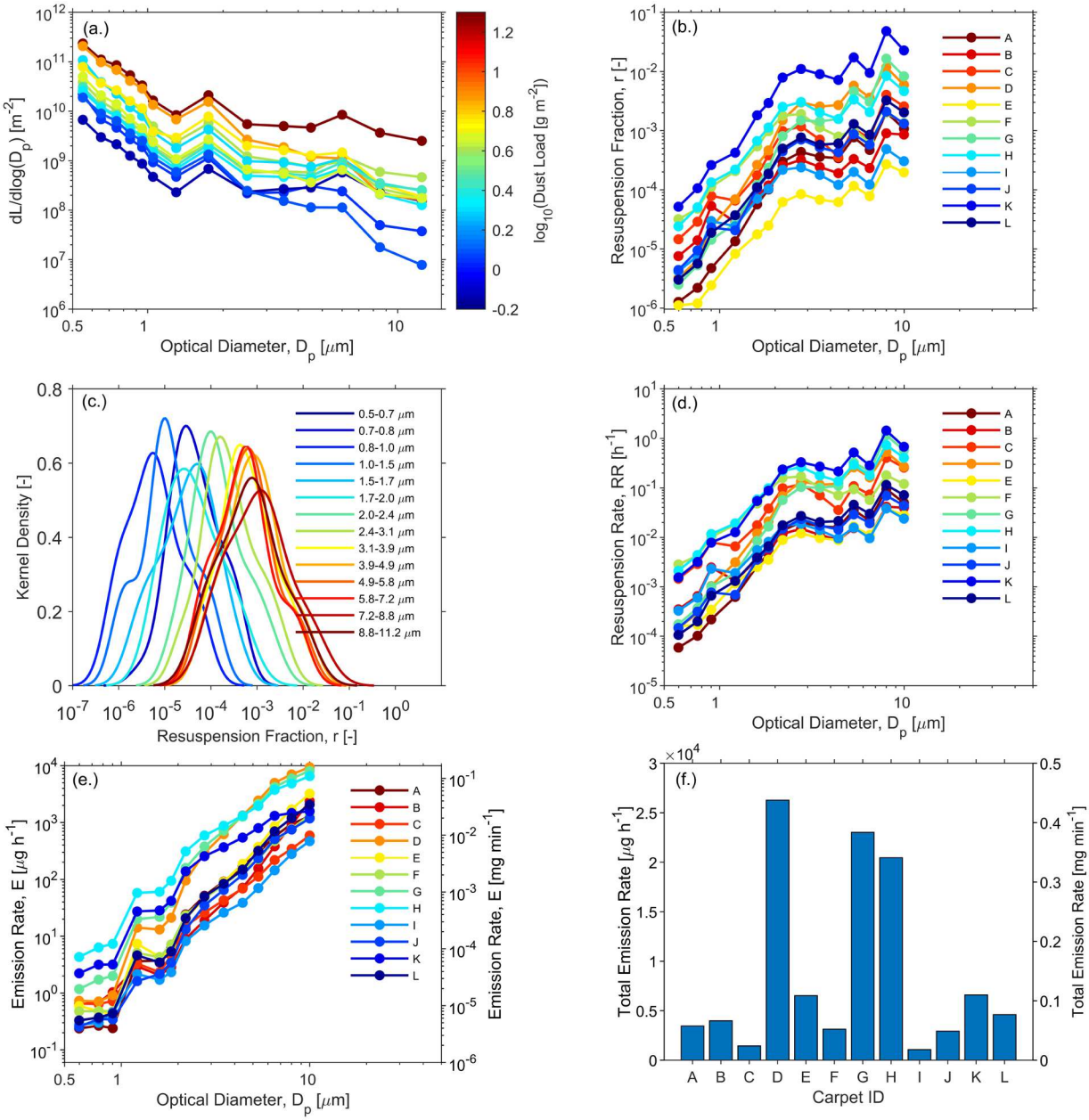

Figure 4. (a) Particle number size distributions in the SD zone ($dL/d\log D_p$, m^{-2}) for each carpet (A–L) with the color of the curves defined by the $\log_{10}$(dust load, g m^{-2}) heat map; (b) mean size-resolved resuspension fractions (r, -) for each carpet (A–L); (c) kernel density estimates of size-resolved resuspension fractions (r, -) across all carpets (A–L); (d) mean size-resolved resuspension rates (RR, h^{-1}) for each carpet (A–L); (e) mean size-resolved particle mass emission rates (E, $\mu g\ h^{-1}$ and mg min^{-1}) for each carpet (A–L); and (f) mean size-integrated (total) particle mass emission rates ($\mu g\ h^{-1}$ and mg min^{-1}) for each carpet (A–L). Values for all parameters for each carpet and size fraction can be found in Tables S4–S9.

small difference between the breathing zone and room-averaged concentrations, while less intensive activities, such as sitting, result in a notable personal cloud effect.[1] The robotic infant did not generate a buoyant thermal plume like a real infant that can aid air mixing, which also contributes to the nonuniform spatial distribution. Since air mixing in real indoor environments is likely weaker than in the chamber (where two BA mixing fans were used), the spatial variation in the concentration of resuspended particles may be more significant.

The vertical distribution of resuspended particles and the personal cloud effect indicate that particle measurements in the BA may underestimate infants' inhalation exposure in the NF microzone. Similar results were observed by Shalat el al.,[92,93] who conducted simultaneous measurements in a young child's breathing zone with a Pretoddler Inhalable Particulate Environmental Robotic (PIPER) sampler and the BA with a stationary monitor. By simulating the activities of young children, the PIPER sampler detected 1.12-fold and 2.3-fold greater mass concentrations of resuspended particles compared to the stationary monitor for bare floors and carpets, respectively.[92] The vertical distribution in particle concentrations was also found for walking-induced resuspension. A resuspension modeling study by Khare and Marr[94] indicates that walking can generate a turbulent wake with a vertical velocity gradient, which can cause a stratified concentration

https://dx.doi.org/10.1021/acs.est.0c06157
Environ. Sci. Technol. 2021, 55, 1864–1875

gradient of resuspended viruses, with the concentration at 1 m above the floor higher than at 2 m by up to 40%.

Impact of Vacuuming on Infant Exposure to Resuspended Particles. The impact of vacuuming on infant exposure to resuspended particles was investigated by comparing the mean concentration in the NF microzone during the crawling period before and after a single vacuuming event. Size-resolved fractional vacuumed reductions for concentrations in the NF microzone are presented for the 12 carpets in Figure 3b. The fractional reduction shows a strong variation among carpets. A notable reduction in resuspended particle concentrations was observed after vacuuming, with fractional reductions ranging from 0.3 to >0.9 for most carpets. Carpet D exhibits the highest fractional reduction, with values ranging from 0.79 to 0.95 across the measured size range. A strong size-dependency in the fractional reduction was found for most carpets, with values increasing with particle size. This indicates that the removal efficiency of SD is size-dependent and that larger particles are more efficiently removed from the carpet during vacuuming. This can be explained by the mechanisms of particle detachment from surfaces, which suggest that the ratio of removal forces to adhesion forces increases with particle size.[95] It is also possible that larger particle agglomerates structurally decompose into several small particles because of the agitation imposed by vacuuming, thus contributing to the size-dependence of the fractional reduction. Contrary to the high fractional reductions observed here for most of the carpets, Roberts et al.[97] and Qian et al.[74] reported low removal efficiencies of SD by vacuuming.

Interestingly, the fractional reduction shows negative values for carpets A and B for certain size ranges, indicating that vacuuming increased, rather than decreased, the concentrations of resuspended particles in the NF microzone. A possible reason for this effect is that the deeply embedded particles were transported upward and closer to the surface of the carpet fiber canopy after the agitation of vacuuming, which makes them more readily available for resuspension. Sercombe et al.[90] demonstrated the existence of the vertical distribution of dust-bound Der p 1 allergen in carpet and indicated that vacuum cleaning can disturb the vertical distribution but not necessarily reduce the total allergen content. In addition, larger particles that were broken down during vacuuming may significantly increase the number of resuspendable smaller particles, resulting in the increasing effect for certain size ranges for carpets A and B.

SD Size Distributions and Size-Resolved Resuspension Fractions. Figure 4a presents the number size distributions of the SD ($dL/d\log D_p$, m^{-2}) collected from each carpet. The color scheme of the size distributions indicates the dust load for each carpet as determined by gravimetric methods. The number size distributions of the SD are similar in shape; a decreasing trend with the increase of particle size can be observed among all carpets. Their magnitude decreases more than 10-fold from $D_p \sim 0.5$ μm to $D_p \sim 11$ μm. A greater number of submicron particles can be observed in the SD, although they contribute marginally to the dust mass loading. A hump can be observed at $D_p \sim 1.8$ μm in the number size distributions, which may be associated with the microbial content of the SD.[15,81,82,96]

Although the number size distributions of the SD present similarity in shape, the variation in magnitude is dramatic among the carpets. For example, the SD on carpet E, with the highest dust load of 19.74 g m^{-2}, exhibits a number size distribution nearly 2 orders of magnitude greater than that for carpet F, which has the lowest dust load of 0.72 g m^{-2}. Generally, as the dust load increases, the magnitude of the number size distribution of SD also increases. The prominent variations in the size distribution of the SD may be attributed to differences in carpet usage and cleaning patterns in the home, indoor particle sources, track-in,[2,71,98] and material/structure of the carpet.

The number size distribution of the SD is essential for estimating size-resolved resuspension fractions (eq S7), a dimensionless measure that represents the fraction of settled particles released from a surface by one stroke of a repetitive contact motion.[2,6,71] The robotic infant simulated the crawling motion by swinging the arms up and down in front of the upper body, and the contact between the hand and the carpet propels the robotic infant forward. Therefore, the resuspension fraction was estimated as the fraction of particles resuspended per swing of the arm or per contact between the hand and the carpet.

Figure 4b presents the mean size-resolved resuspension fractions for each carpet. The resuspension fraction exhibits more than 2 orders of magnitude variation across the 12 carpets for a given particle size. The crawling-induced resuspension fraction varies widely, from 10^{-6} to 10^{-1} across the measured size range. Intercarpet variations are better visualized in Figure 4c, which presents the kernel density estimates of size-resolved resuspension fractions among all carpets. For each size bin, the kernel density curve presents a wide peak, spanning over 2 orders of magnitude.

The significant intercarpet variation in resuspension fractions may be attributed to the difference in density, construction, age, and material of the carpet, intrinsic properties of the settled particles, and variations in relative humidity during the experiments. For example, cut-pile carpets with a low fiber density could result in 1.5−2.5 times higher resuspension fractions than those with a high fiber density.[4] Tian et al.[4] have attributed this finding to the improved ability of high-density carpets to hold the fibers in a vertical orientation, while low-density fibers tend to bend more readily. High-density cut-pile carpets could have higher resuspension fractions compared to high-density loop carpets because of the greater vertical compression of the carpet fibers.[4,85] Old and worn carpets may result in a lower resuspension fraction because of changes in their abilities to spring back and the accumulation of "sticky" materials.[83] Different carpet materials can lead to different particle-to-carpet adhesion forces, further affecting the resuspension fraction. Previous measurements by atomic force microscopy indicate that the adhesion forces between polystyrene and *Escherichia coli* are on average 1.4 times greater than those between polyamide and *E. coli*.[84] The settled particles on each carpet may originate from different sources, thereby adopting different intrinsic properties[6] that affect particle removal and adhesion forces.[99−105] Relative humidity influences the amount of condensed water between the particle and the carpet fiber, thus affecting adhesion by capillary forces.[106−110] It also changes the conductivity of the settled particle, which affects the electrostatic force.[110] However, the relative humidity varied across a relatively narrow range during the experiments (Table S1); therefore, it may not contribute significantly to the intercarpet variations in resuspension fractions.

The size-resolved resuspension fractions present an increasing trend with particle size among all carpets, which is

https://dx.doi.org/10.1021/acs.est.0c06157
Environ. Sci. Technol. 2021, 55, 1864−1875

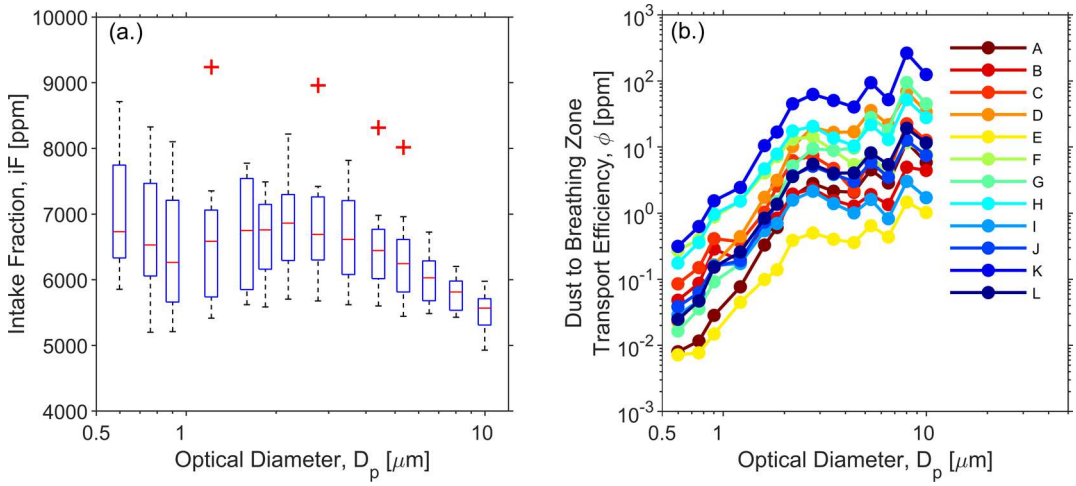

Figure 5. (a) Size-resolved intake fractions (iFs, ppm) for all carpets and (b) size-resolved dust-to-breathing zone transport efficiencies (Φ, ppm) for each carpet (A–L). For (a), box plots represent the interquartile range, whiskers represent the 5th and 95th percentiles, and markers represent outliers. Data for all carpets were compiled. Values for iF and Φ for each carpet and size fraction can be found in Tables S10 and S11, respectively.

consistent with previous studies of adult walking-induced resuspension. This is because the ratio of removal forces to adhesion forces increases with particle size.[95] The resuspension fractions induced by an adult walking on carpets are in the range of 10^{-6} to 5×10^{-2} for particles from D_p = 0.4 to 10 μm.[2,4,6,71] The crawling-induced resuspension simulated by the robotic infant presents values in a similar range. However, the mechanisms of resuspension induced by the robotic infant on carpets are somewhat different from those caused by adults performing upright walking locomotion. First, the adult can be physically stronger than the robotic infant. The strength of waving arms by the robotic infant is expected to be weaker than that of adult footfalls during walking, and the projected area of the mechanical arm is expected to be smaller than the foot of an adult. Therefore, the air jet generated by the waving arm might be weaker than that generated by the footfall. Thus, contributions by aerodynamic forces to resuspension may be less than that for adults. Second, although the resuspension fractions were estimated as per swing of the arm or per contact between the hand and the carpet, the contact between the lower torso and the carpet also contributes to resuspension. As the swinging arm propels the robotic infant forward, the lower torso is dragged along the carpet, which can cause compression/decompression of the carpet fibers. This process can induce particle resuspension; however, it is difficult to be accounted for when estimating the resuspension fraction as per stroke of movement.[6] Third, as the surface of the robotic infant was covered with a grounded aluminum tape, electrostatic forces likely contribute negligibly to resuspension. Therefore, in this study, the main mechanisms related to crawling-induced resuspension are aerodynamic drag/lift and mechanical vibration of the carpet fibers.

Figure 4d presents the mean size-resolved resuspension rates (h^{-1}),[2,6,74] which represent the fraction of settled particles removed from the carpet per unit time. The resuspension rate spans from 10^{-5} to 1 h^{-1} for particles from D_p = 0.5 to 11 μm, with the same trend as the resuspension fraction. Assuming a resuspended particle will not deposit back to the carpet, the reciprocal of the resuspension rate is the timescale needed to deplete all settled particles on the carpet by resuspension. The values of the reciprocals are within the range from 10^2 to 10^4 h for submicron particles, indicating that the carpet can serve as a sustainable source for resuspension which cannot be depleted in-practice. As the particle size increases, the resuspension rate increases by 2 orders of magnitude, while values of the reciprocals can drop by 2 orders of magnitude, meaning much shorter periods are needed to deplete larger particles from the surface. The reciprocal of the resuspension rate varies from 0.5 to 100 h for D_p > 7 μm. Thus, the dust load on some of the carpets can decrease relatively fast and the concentration of resuspended particles in this size range may drop after a long period of continuous crawling or physical disturbance.

Size-Resolved and Size-Integrated Emission Rates. The mean size-resolved particle mass emission rates during the crawling periods (Figure 4e) present similar profiles as the mass size distributions (Figure 2b). Size-resolved emission rates ranged from 10^{-1} to 10^4 μg h^{-1} (10^{-6} to 10^{-1} mg min^{-1}) and are similar to those from the resuspension induced by a mechanical foot reported by Tian et al.[4] but lower than the values reported for an adult walking by Thatcher and Layton,[71] Ferro et al.,[111] Qian et al.,[74] Qian and Ferro,[2] and Rosati et al.[83] The mean size-integrated mass emission rates for most carpets vary between 1 and 5×10^3 μg h^{-1}, with values exceeding 2×10^4 for carpets D, G, and H. The size-integrated mass emission rate on each carpet did not exhibit a clear relationship with the dust load. For example, carpet E has the highest dust load of 19.74 g m^{-2}, but the size-integrated mass emission rate is the fifth highest among all carpets.

Size-Resolved Inhalation Intake Fractions and Dust-to-Breathing Zone Transport Efficiencies. As a metric to further characterize an infant's inhalation exposure to resuspended particles, the intake fraction, iF, which considers the factors involved in the source-receptor transport process, was calculated as a function of particle size. Since the infant may be exposed to resuspended particles during both crawling and decay periods, the iF was calculated as the ratio of the number of particles inhaled during both periods to the number of particles resuspended during the crawling period (eq S10). The size-resolved iFs from the resuspension experiments across all carpets were compiled and are presented as box plots in Figure 5a. The median inhalation iF ranges from 5.6×10^3 to 6.9×10^3 ppm between D_p = 0.517 and 11.2 μm, indicating that more than 0.5% of the resuspended particles can be inhaled by a crawling infant. These values are within the range

https://dx.doi.org/10.1021/acs.est.0c06157
Environ. Sci. Technol. 2021, 55, 1864–1875

of previously reported iFs for different indoor emission sources.[3,65,112]

The size-resolved iFs decrease with increasing particle size from $D_p \sim 0.5$ to 1 μm and from $D_p \sim 2$ to 11 μm. This is likely due to the increase in the deposition rate with particle size, causing a greater fraction of smaller particles to remain suspended for a longer period, increasing the probability of inhalation. Similar trends were also observed by Boor et al.[3] and Licina et al.[65] Interestingly, a local maximum in the size-resolved intake fraction is present between $D_p \sim 2$ and 3 μm. Although the reason is unclear, Licina et al.[65] also showed a similar mode between $D_p \sim 1$ and 3 μm when estimating the intake fraction by using a heated manikin with point sources emitted near the feet or groin. The mode between $D_p \sim 2$ and 3 μm in the size-resolved iF overlaps with the peak of the number size distribution of resuspended fluorescent biological aerosol particles from carpets,[15,20,82] which was found to be associated with bacterial agglomerates and fungal spores.[15,20,21,113,114]

While the intake fraction is certainly useful for inhalation exposure assessment, the new metric defined in this paper, the dust-to-breathing zone transport efficiency (Φ), is of greater value since it lumps two key physical processes related to inhalation exposure together: resuspension from the carpet and delivery of resuspended particles to the human respiratory airways. Φ takes both the resuspension fraction and intake fraction into consideration (eq S12). The former accounts for the balance between removal and adhesion forces, which is the essential determinant of particle resuspension, while the latter accounts for the fate and transport of the resuspended particles, which determines if a resuspended particle can be inhaled. Thus, the value of Φ represents the overall likelihood of a settled particle being resuspended and inhaled by a crawling infant.

The value of Φ ranges from 0.01 to 263 ppm for particles between $D_p = 0.517$ and 11.2 μm across the 12 carpets (Figure 5b). The intercarpet variation of Φ is pronounced, which spans over 2 orders of magnitude. Since the chamber ventilation conditions and the locomotion of the robotic infant remain the same during the experiments, this finding indicates that differences in the characteristics of carpets can cause a significant variation in Φ. In general, Φ exhibits an increasing trend with particle size, increasing by 2 orders of magnitude from $D_p = 0.517$ to $D_p = 11.2$ μm. It suggests that larger SD particles are more likely to be resuspended and inhaled per disturbance by infants during crawling as compared to smaller particles. While the value of Φ is a combination of the resuspension and intake fractions, the profile of the size-resolved Φ resembles that of the resuspension fraction rather than that of the intake fraction. This indicates that the resuspension fraction has a greater influence on Φ. This is because of the stronger size-dependence of the resuspension fraction, which varies by more than 2 orders of magnitude across the measured size range, while the iF only varies by a factor less than 2.

Infant Exposure to Resuspended Carpet Dust in Real Scenarios. This study evaluates an infant's exposure to crawling-induced resuspended particles from carpets by using a robotic infant performing a belly crawl in a repeatable manner. This simplified crawling locomotion can only serve as an example to illustrate how infants are exposed to self-induced resuspended particles. In reality, their exposure in the NF microzone is more complicated because of the complexity of infants' movements. First, how well the robotic infant can mimic the crawling locomotion of an infant is unknown. The frequency, area, and strength of contact and the pattern of locomotion will all affect the resuspension process. Discrepancies between simulated and real crawling behaviors will induce some uncertainties in the exposure characterization presented in this study. The mechanisms of crawling-induced resuspension need to be further investigated. Second, infants are exposed to particles by other activities beyond crawling. Playing, walking, and rolling will also induce resuspension. Third, the movements of infants are highly transient with constantly changing activity types, suggesting temporally variant resuspension and exposure events. Fourth, the factors that influence infants' activities, such as age and locomotion experience,[7,8,12,115] are also expected to affect dust resuspension and exposure. This study provides a methodology to investigate the infant crawling-induced resuspension process in a controlled environment. Such an approach can be applied to similar studies to evaluate the influence of individual factors on particle resuspension, such as dust load, carpet type, and carpet material with artificially seeded carpets. The resuspension and inhalation parameters estimated in this study can be used for modeling studies to predict inhalation exposure to particular chemical contaminants or microbes of concern.

■ ASSOCIATED CONTENT

Supporting Information

The Supporting Information is available free of charge at https://pubs.acs.org/doi/10.1021/acs.est.0c06157.

Detailed materials and methods section, details on the three-zone material balance model, influence of carpet type on resuspension, study limitations, and other SI figures and tables mentioned herein (PDF)

■ AUTHOR INFORMATION

Corresponding Author

Brandon E. Boor − *Lyles School of Civil Engineering and Ray W. Herrick Laboratories, Center for High Performance Buildings, Purdue University, West Lafayette, Indiana 47907, United States;* orcid.org/0000-0003-1011-4100; Email: bboor@purdue.edu

Authors

Tianren Wu − *Lyles School of Civil Engineering and Ray W. Herrick Laboratories, Center for High Performance Buildings, Purdue University, West Lafayette, Indiana 47907, United States*

Manjie Fu − *Ray W. Herrick Laboratories, Center for High Performance Buildings and Weldon School of Biomedical Engineering, Purdue University, West Lafayette, Indiana 47907, United States*

Maria Valkonen − *Environmental Health Unit, Finnish Institute for Health and Welfare, Kuopio 70701, Finland*

Martin Täubel − *Environmental Health Unit, Finnish Institute for Health and Welfare, Kuopio 70701, Finland;* orcid.org/0000-0001-8082-1041

Ying Xu − *Department of Building Science, Tsinghua University, Beijing 100084, China;* orcid.org/0000-0002-1908-7981

Complete contact information is available at: https://pubs.acs.org/10.1021/acs.est.0c06157

https://dx.doi.org/10.1021/acs.est.0c06157
Environ. Sci. Technol. 2021, 55, 1864−1875

Notes

The authors declare no competing financial interest.

■ ACKNOWLEDGMENTS

We thank the families who donated their carpets to this study, Rauno Holopainen for his assistance with the operation of the environmental chamber used in the resuspension experiments, and Sinikka Vainiotalo for her assistance with the gravimetric measurements of collected carpet dust. Financial support was provided by the National Science Foundation (CBET-1805804), The Academy of Finland (PROBIOM: 296814 and 296817), and Juho Vainion Säätiö (201710468).

■ REFERENCES

(1) Licina, D.; Tian, Y.; Nazaroff, W. W. Emission Rates and the Personal Cloud Effect Associated with Particle Release from the Perihuman Environment. *Indoor Air* **2017**, *27*, 791−802.
(2) Qian, J.; Ferro, A. R. Resuspension of Dust Particles in a Chamber and Associated Environmental Factors. *Aerosol Sci. Technol.* **2008**, *42*, 566−578.
(3) Boor, B. E.; Spilak, M. P.; Corsi, R. L.; Novoselac, A. Characterizing Particle Resuspension from Mattresses: Chamber Study. *Indoor Air* **2015**, *25*, 441−456.
(4) Tian, Y.; Sul, K.; Qian, J.; Mondal, S.; Ferro, A. R. A Comparative Study of Walking-induced Dust Resuspension Using a Consistent Test Mechanism. *Indoor Air* **2014**, *24*, 592−603.
(5) Boor, B. E.; Siegel, J. A.; Novoselac, A. Wind Tunnel Study on Aerodynamic Particle Resuspension from Monolayer and Multilayer Deposits on Linoleum Flooring and Galvanized Sheet Metal. *Aerosol Sci. Technol.* **2013**, *47*, 848−857.
(6) Qian, J.; Peccia, J.; Ferro, A. R. Walking-Induced Particle Resuspension in Indoor Environments. *Atmos. Environ.* **2014**, *89*, 464−481.
(7) Badaly, D.; Adolph, K. E. Beyond the Average: Walking Infants Take Steps Longer than Their Leg Length. *Infant Behav. Dev.* **2008**, *31*, 554−558.
(8) Adolph, K.; Eppler, M. Development of Visually Guided Locomotion. *Ecol. Psychol.* **1998**, *10*, 303−321.
(9) Adolph, K. E.; Vereijken, B.; Denny, M. A. Learning to Crawl. *Child Dev.* **1998**, *69*, 1299−1312.
(10) Adolph, K. E.; Cole, W. G.; Komati, M.; Garciaguirre, J. S.; Badaly, D.; Lingeman, J. M.; Chan, G. L. Y.; Sotsky, R. B. How Do You Learn to Walk? Thousands of Steps and Dozens of Falls per Day. *Psychol. Sci.* **2012**, *23*, 1387−1394.
(11) Adolph, K. E.; Tamis-LeMonda, C. S. The Costs and Benefits of Development: The Transition from Crawling to Walking. *Child Dev. Perspect.* **2014**, *8*, 187−192.
(12) Adolph, K. E.; Eppler, M. A. Flexibility and Specificity in Infant Motor Skill Acquisition. *Progress in Infancy Research*; Psychology Press, 2002; pp 147−194.
(13) Team, D. Datavyu: A Video Coding Tool. Databrary Project; New York University. 2014, http//datavyu.org.
(14) Hoch, J. E.; O'Grady, S. M.; Adolph, K. E. It's the Journey, Not the Destination: Locomotor Exploration in Infants. *Dev. Sci.* **2019**, *22*, No. e12740.
(15) Wu, T.; Täubel, M.; Holopainen, R.; Viitanen, A.-K.; Vainiotalo, S.; Tuomi, T.; Keskinen, J.; Hyvärinen, A.; Hämeri, K.; Saari, S. E.; Boor, B. E. Infant and Adult Inhalation Exposure to Resuspended Biological Particulate Matter. *Environ. Sci. Technol.* **2018**, *52*, 237−247.
(16) Dannemiller, K. C.; Mendell, M. J.; Macher, J. M.; Kumagai, K.; Bradman, A.; Holland, N.; Harley, K.; Eskenazi, B.; Peccia, J. Next-generation DNA Sequencing Reveals That Low Fungal Diversity in House Dust Is Associated with Childhood Asthma Development. *Indoor Air* **2014**, *24*, 236−247.
(17) Dannemiller, K. C.; Gent, J. F.; Leaderer, B. P.; Peccia, J. Indoor Microbial Communities: Influence on Asthma Severity in Atopic and Nonatopic Children. *J. Allergy Clin. Immunol.* **2016**, *138*, 76−83.
(18) Chew, G. L.; Rogers, C.; Burge, H. A.; Muilenberg, M. L.; Gold, D. R. Dustborne and Airborne Fungal Propagules Represent a Different Spectrum of Fungi with Differing Relations to Home Characteristics. *Allergy* **2003**, *58*, 13−20.
(19) Chew, G. L.; Burge, H. A.; Dockery, D. W.; Muilenberg, M. L.; Weiss, S. T.; Gold, D. R. Limitations of a Home Characteristics Questionnaire as a Predictor of Indoor Allergen Levels. *Am. J. Respir. Crit. Care Med.* **1998**, *157*, 1536−1541.
(20) Hyytiäinen, H. K.; Jayaprakash, B.; Kirjavainen, P. V.; Saari, S. E.; Holopainen, R.; Keskinen, J.; Hämeri, K.; Hyvärinen, A.; Boor, B. E.; Täubel, M. Crawling-Induced Floor Dust Resuspension Affects the Microbiota of the Infant Breathing Zone. *Microbiome* **2018**, *6*, 25.
(21) Adams, R. I.; Bhangar, S.; Pasut, W.; Arens, E. A.; Taylor, J. W.; Lindow, S. E.; Nazaroff, W. W.; Bruns, T. D. Chamber Bioaerosol Study: Outdoor Air and Human Occupants as Sources of Indoor Airborne Microbes. *PLoS One* **2015**, *10*, No. e0128022.
(22) Kissa, E. *Fluorinated Surfactants and Repellents*; CRC Press, 2001; Vol. *97*.
(23) Prevedouros, K.; Cousins, I. T.; Buck, R. C.; Korzeniowski, S. H. Sources, Fate and Transport of Perfluorocarboxylates. *Environ. Sci. Technol.* **2006**, *40*, 32−44.
(24) Kubwabo, C.; Stewart, B.; Zhu, J.; Marro, L. Occurrence of Perfluorosulfonates and Other Perfluorochemicals in Dust from Selected Homes in the City of Ottawa, Canada. *J. Environ. Monit.* **2005**, *7*, 1074−1078.
(25) Petersen, R. C. Triclosan Antimicrobial Polymers. *AIMS Mol. Sci.* **2016**, *3*, 88.
(26) Langer, S.; Weschler, C. J.; Fischer, A.; Bekö, G.; Toftum, J.; Clausen, G. Phthalate and PAH Concentrations in Dust Collected from Danish Homes and Daycare Centers. *Atmos. Environ.* **2010**, *44*, 2294−2301.
(27) Curits, K.; Wilding, B. C.; Hulick, A.; LaBo, K.; Schuler, K. Flame retardants in furniture, foam, floors. https://www.conservationminnesota.org/redesign/wp-content/uploads/SafeMattressReport-final.pdf (accessed August 19, 2015).
(28) Qi, H.; Li, W.-L.; Zhu, N.-Z.; Ma, W.-L.; Liu, L.-Y.; Zhang, F.; Li, Y.-F. Concentrations and Sources of Polycyclic Aromatic Hydrocarbons in Indoor Dust in China. *Sci. Total Environ.* **2014**, *491*−*492*, 100−107.
(29) Vostal, J. J.; Taves, E.; Sayre, J. W.; Charney, E. Lead Analysis of the House Dust: A Method for the Detection of Another Source of Lead Exposure in Inner City Children. *Environ. Health Perspect.* **1974**, *7*, 91−97.
(30) Bornschein, R. L.; Succop, P. A.; Krafft, K. M.; Clark, C. S.; Peace, B.; Hammond, P. B. *Exterior Surface Dust Lead, Interior House Dust Lead and Childhood Lead Exposure in an Urban Environment*; University of Cincinnati: OH, 1986.
(31) Lanphear, B. P.; Matte, T. D.; Rogers, J.; Clickner, R. P.; Dietz, B.; Bornschein, R. L.; Succop, P.; Mahaffey, K. R.; Dixon, S.; Galke, W.; Rabinowitz, M.; Farfel, M.; Rohde, C.; Schwartz, J.; Ashley, P.; Jacobs, D. E. The Contribution of Lead-Contaminated House Dust and Residential Soil to Children's Blood Lead Levels. *Environ. Res.* **1998**, *79*, 51−68.
(32) Madany, I. M.; Salim Akhter, M.; Al Jowder, O. A. The Correlations between Heavy Metals in Residential Indoor Dust and Outdoor Street Dust in Bahrain. *Environ. Int.* **1994**, *20*, 483−492.
(33) Zheng, J.; Chen, K.-h.; Yan, X.; Chen, S.-J.; Hu, G.-C.; Peng, X.-W.; Yuan, J.-g.; Mai, B.-X.; Yang, Z.-Y. Heavy Metals in Food, House Dust, and Water from an e-Waste Recycling Area in South China and the Potential Risk to Human Health. *Ecotoxicol. Environ. Saf.* **2013**, *96*, 205−212.
(34) Akhter, M. S.; Madany, I. M. Heavy Metals in Street and House Dust in Bahrain. *Water, Air, Soil Pollut.* **1993**, *66*, 111−119.
(35) Torrent, M.; Sunyer, J.; Muñoz, L.; Cullinan, P.; Iturriaga, M.; Figueroa, C.; Vall, O.; Taylor, A.; Anto, J. Early-Life Domestic Aeroallergen Exposure and IgE Sensitization at Age 4 Years. *J. Allergy Clin. Immunol.* **2006**, *118*, 742−748.

https://dx.doi.org/10.1021/acs.est.0c06157
Environ. Sci. Technol. 2021, 55, 1864−1875

(36) Sporik, R.; Holgate, S. T.; Platts-Mills, T. A. E.; Cogswell, J. J. Exposure to House-Dust Mite Allergen (Der p I) and the Development of Asthma in Childhood: A Prospective Study. *N. Engl. J. Med.* **1990**, *323*, 502−507.
(37) Gehring, U.; Bischof, W.; Fahlbusch, B.; Wichmann, H.-E.; Heinrich, J. House Dust Endotoxin and Allergic Sensitization in Children. *Am. J. Respir. Crit. Care Med.* **2002**, *166*, 939−944.
(38) Méheust, D.; Le Cann, P.; Reboux, G.; Millon, L.; Gangneux, J.-P. Indoor Fungal Contamination: Health Risks and Measurement Methods in Hospitals, Homes and Workplaces. *Crit. Rev. Microbiol.* **2014**, *40*, 248−260.
(39) Calderón, M. A.; Linneberg, A.; Kleine-Tebbe, J.; De Blay, F.; Hernandez Fernandez de Rojas, D.; Virchow, J. C.; Demoly, P. Respiratory Allergy Caused by House Dust Mites: What Do We Really Know? *J. Allergy Clin. Immunol.* **2015**, *136*, 38−48.
(40) Denning, D. W.; O'driscoll, B. R.; Hogaboam, C. M.; Bowyer, P.; Niven, R. M. The Link between Fungi and Severe Asthma: A Summary of the Evidence. *Eur. Respir. J.* **2006**, *27*, 615−626.
(41) Dannemiller, K. C.; Gent, J. F.; Leaderer, B. P.; Peccia, J. Influence of Housing Characteristics on Bacterial and Fungal Communities in Homes of Asthmatic Children. *Indoor Air* **2016**, *26*, 179−192.
(42) Thorne, P. S.; Kulhánková, K.; Yin, M.; Cohn, R.; Arbes, S. J., Jr; Zeldin, D. C. Endotoxin Exposure Is a Risk Factor for Asthma. *Am. J. Respir. Crit. Care Med.* **2005**, *172*, 1371−1377.
(43) Heinrich, J.; Gehring, U.; Douwes, J.; Koch, A.; Fahlbusch, B.; Bischof, W.; Wichmann, H. E. Pets and Vermin Are Associated with High Endotoxin Levels in House Dust. *Clin. Exp. Allergy* **2001**, *31*, 1839−1845.
(44) Bonvallot, N.; Mandin, C.; Mercier, F.; Le Bot, B.; Glorennec, P. Health Ranking of Ingested Semi-volatile Organic Compounds in House Dust: An Application to France. *Indoor Air* **2010**, *20*, 458−472.
(45) Park, J.-H.; Gold, D. R.; Spiegelman, D. L.; Burge, H. A.; Milton, D. K. House Dust Endotoxin and Wheeze in the First Year of Life. *Am. J. Respir. Crit. Care Med.* **2001**, *163*, 322−328.
(46) Von Mutius, E.; Vercelli, D. Farm Living: Effects on Childhood Asthma and Allergy. *Nat. Rev. Immunol.* **2010**, *10*, 861−868.
(47) Ege, M. J.; Mayer, M.; Normand, A.-C.; Genuneit, J.; Cookson, W. O. C. M.; Braun-Fahrländer, C.; Heederik, D.; Piarroux, R.; von Mutius, E. Exposure to Environmental Microorganisms and Childhood Asthma. *N. Engl. J. Med.* **2011**, *364*, 701−709.
(48) Valkonen, M.; Wouters, I. M.; Täubel, M.; Rintala, H.; Lenters, V.; Vasara, R.; Genuneit, J.; Braun-Fahrländer, C.; Piarroux, R.; Von Mutius, E. Bacterial Exposures and Associations with Atopy and Asthma in Children. *PLoS One* **2015**, *10*, No. e0131594.
(49) Tovey, E. R.; Almqvist, C.; Li, Q.; Crisafulli, D.; Marks, G. B. Nonlinear Relationship of Mite Allergen Exposure to Mite Sensitization and Asthma in a Birth Cohort. *J. Allergy Clin. Immunol.* **2008**, *122*, 114−118.
(50) Tischer, C.; Weikl, F.; Probst, A. J.; Standl, M.; Heinrich, J.; Pritsch, K. Urban Dust Microbiome: Impact on Later Atopy and Wheezing. *Environ. Health Perspect.* **2016**, *124*, 1919−1923.
(51) Stein, M. M.; Hrusch, C. L.; Gozdz, J.; Igartua, C.; Pivniouk, V.; Murray, S. E.; Ledford, J. G.; Marques dos Santos, M.; Anderson, R. L.; Metwali, N.; Neilson, J. W.; Maier, R. M.; Gilbert, J. A.; Holbreich, M.; Thorne, P. S.; Martinez, F. D.; von Mutius, E.; Vercelli, D.; Ober, C.; Sperling, A. I. Innate Immunity and Asthma Risk in Amish and Hutterite Farm Children. *N. Engl. J. Med.* **2016**, *375*, 411−421.
(52) Peters, M.; Kauth, M.; Scherner, O.; Gehlhar, K.; Steffen, I.; Wentker, P.; von Mutius, E.; Holst, O.; Bufe, A. Arabinogalactan Isolated from Cowshed Dust Extract Protects Mice from Allergic Airway Inflammation and Sensitization. *J. Allergy Clin. Immunol.* **2010**, *126*, 648−656.
(53) Lawson, J. A.; Dosman, J. A.; Rennie, D. C.; Beach, J. R.; Newman, S. C.; Crowe, T.; Senthilselvan, A. Endotoxin as a Determinant of Asthma and Wheeze among Rural Dwelling Children and Adolescents: A Case−Control Study. *BMC Pulm. Med.* **2012**, *12*, 56.
(54) Lynch, S. V.; Wood, R. A.; Boushey, H.; Bacharier, L. B.; Bloomberg, G. R.; Kattan, M.; O'Connor, G. T.; Sandel, M. T.; Calatroni, A.; Matsui, E.; Johnson, C. C.; Lynn, H.; Visness, C. M.; Jaffee, K. F.; Gergen, P. J.; Gold, D. R.; Wright, R. J.; Fujimura, K.; Rauch, M.; Busse, W. W.; Gern, J. E. Effects of Early-Life Exposure to Allergens and Bacteria on Recurrent Wheeze and Atopy in Urban Children. *J. Allergy Clin. Immunol.* **2014**, *134*, 593−601.
(55) Ege, M. J.; Mayer, M.; Schwaiger, K.; Mattes, J.; Pershagen, G.; Van Hage, M.; Scheynius, A.; Bauer, J.; Von Mutius, E. Environmental Bacteria and Childhood Asthma. *Allergy* **2012**, *67*, 1565−1571.
(56) Misztal, P. K.; Lymperopoulou, D. S.; Adams, R. I.; Scott, R. A.; Lindow, S. E.; Bruns, T.; Taylor, J. W.; Uehling, J.; Bonito, G.; Vilgalys, R.; Goldstein, A. H. Emission Factors of Microbial Volatile Organic Compounds from Environmental Bacteria and Fungi. *Environ. Sci. Technol.* **2018**, *52*, 8272−8282.
(57) Nurmatov, U. B.; Tagiyeva, N.; Semple, S.; Devereux, G.; Sheikh, A. Volatile Organic Compounds and Risk of Asthma and Allergy: A Systematic Review. *Eur. Respir. Rev.* **2015**, *24*, 92−101.
(58) Bönisch, U.; Böhme, A.; Kohajda, T.; Mögel, I.; Schütze, N.; von Bergen, M.; Simon, J. C.; Lehmann, I.; Polte, T. Volatile Organic Compounds Enhance Allergic Airway Inflammation in an Experimental Mouse Model. *PLoS One* **2012**, *7*, No. e39817.
(59) Korpi, A.; Järnberg, J.; Pasanen, A.-L. Microbial Volatile Organic Compounds. *Crit. Rev. Toxicol.* **2009**, *39*, 139−193.
(60) Shan, Y.; Wu, W.; Fan, W.; Haahtela, T.; Zhang, G. House Dust Microbiome and Human Health Risks. *Int. Microbiol.* **2019**, *22*, 297−304.
(61) Haines, S. R.; Siegel, J. A.; Dannemiller, K. C. Modeling Microbial Growth in Carpet Dust Exposed to Diurnal Variations in Relative Humidity Using the "Time-of-Wetness" Framework. *Indoor Air* **2020**, *30*, 978.
(62) Korpi, A.; Pasanen, A.-L.; Pasanen, P.; Kalliokoski, P. Microbial Growth and Metabolism in House Dust. *Int. Biodeterior. Biodegrad.* **1997**, *40*, 19−27.
(63) Hodas, N.; Loh, M.; Shin, H.-M.; Li, D.; Bennett, D.; McKone, T. E.; Jolliet, O.; Weschler, C. J.; Jantunen, M.; Lioy, P.; Fantke, P. Indoor Inhalation Intake Fractions of Fine Particulate Matter: Review of Influencing Factors. *Indoor Air* **2016**, *26*, 836−856.
(64) Fantke, P.; Jolliet, O.; Apte, J. S.; Hodas, N.; Evans, J.; Weschler, C. J.; Stylianou, K. S.; Jantunen, M.; McKone, T. E. Characterizing Aggregated Exposure to Primary Particulate Matter: Recommended Intake Fractions for Indoor and Outdoor Sources. *Environ. Sci. Technol.* **2017**, *51*, 9089−9100.
(65) Licina, D.; Tian, Y.; Nazaroff, W. W. Inhalation Intake Fraction of Particulate Matter from Localized Indoor Emissions. *Build. Environ.* **2017**, *123*, 14−22.
(66) Boor, B. E.; Siegel, J. A.; Novoselac, A. Monolayer and Multilayer Particle Deposits on Hard Surfaces: Literature Review and Implications for Particle Resuspension in the Indoor Environment. *Aerosol Sci. Technol.* **2013**, *47*, 831−847.
(67) Serfozo, N.; Chatoutsidou, S. E.; Lazaridis, M. The Effect of Particle Resuspension during Walking Activity to PM10 Mass and Number Concentrations in an Indoor Microenvironment. *Build. Environ.* **2014**, *82*, 180−189.
(68) Lai, A. C. K.; Tian, Y.; Tsoi, J. Y. L.; Ferro, A. R. Experimental Study of the Effect of Shoes on Particle Resuspension from Indoor Flooring Materials. *Build. Environ.* **2017**, *118*, 251−258.
(69) Gomes, C.; Freihaut, J.; Bahnfleth, W. Resuspension of Allergen-Containing Particles under Mechanical and Aerodynamic Disturbances from Human Walking. *Atmos. Environ.* **2007**, *41*, 5257−5270.
(70) Shaughnessy, R.; Vu, H. Particle Loadings and Resuspension Related to Floor Coverings in Chamber and in Occupied School Environments. *Atmos. Environ.* **2012**, *55*, 515−524.
(71) Thatcher, T.; Layton, D. W. Deposition, Resuspension, and Penetration of Particles within a Residence. *Atmos. Environ.* **1995**, *29*, 1487−1497.

https://dx.doi.org/10.1021/acs.est.0c06157
Environ. Sci. Technol. 2021, 55, 1864−1875

(72) Raja, S.; Xu, Y.; Ferro, A. R.; Jaques, P. A.; Hopke, P. K. Resuspension of Indoor Aeroallergens and Relationship to Lung Inflammation in Asthmatic Children. *Environ. Int.* **2010**, *36*, 8−14.
(73) Oberoi, R. C.; Choi, J.-I.; Edwards, J. R.; Rosati, J. A.; Thornburg, J.; Rodes, C. E. Human-Induced Particle Re-Suspension in a Room. *Aerosol Sci. Technol.* **2010**, *44*, 216−229.
(74) Qian, J.; Ferro, A. R.; Fowler, K. R. Estimating the Resuspension Rate and Residence Time of Indoor Particles. *J. Air Waste Manage. Assoc.* **2008**, *58*, 502−516.
(75) Cherrie, J. W. The Effect of Room Size and General Ventilation on the Relationship between near and Far-Field Concentrations. *Appl. Occup. Environ. Hyg.* **1999**, *14*, 539−546.
(76) Jayjock, M. A.; Armstrong, T.; Taylor, M. The Daubert Standard as Applied to Exposure Assessment Modeling Using the Two-Zone (NF/FF) Model Estimation of Indoor Air Breathing Zone Concentration as an Example. *J. Occup. Environ. Hyg.* **2011**, *8*, D114−D122.
(77) Earnest, C. M.; Corsi, R. L. Inhalation Exposure to Cleaning Products: Application of a Two-Zone Model. *J. Occup. Environ. Hyg.* **2013**, *10*, 328−335.
(78) Koivisto, A. J.; Jensen, A. C. Ø.; Levin, M.; Kling, K. I.; Maso, M. D.; Nielsen, S. H.; Jensen, K. A.; Koponen, I. K. Testing the near Field/Far Field Model Performance for Prediction of Particulate Matter Emissions in a Paint Factory. *Environ. Sci.: Processes Impacts* **2015**, *17*, 62−73.
(79) Zhang, Y.; Banerjee, S.; Yang, R.; Lungu, C.; Ramachandran, G. Bayesian Modeling of Exposure and Airflow Using Two-Zone Models. *Ann. Occup. Hyg.* **2009**, *53*, 409−424.
(80) Cherrie, J. W.; Maccalman, L.; Fransman, W.; Tielemans, E.; Tischer, M.; Van Tongeren, M. Revisiting the Effect of Room Size and General Ventilation on the Relationship between Near-and Far-Field Air Concentrations. *Ann. Occup. Hyg.* **2011**, *55*, 1006−1015.
(81) Bhangar, S.; Huffman, J. A.; Nazaroff, W. W. Size-Resolved Fluorescent Biological Aerosol Particle Concentrations and Occupant Emissions in a University Classroom. *Indoor Air* **2014**, *24*, 604.
(82) Bhangar, S.; Adams, R. I.; Pasut, W.; Huffman, J. A.; Arens, E. A.; Taylor, J. W.; Bruns, T. D.; Nazaroff, W. W. Chamber Bioaerosol Study: Human Emissions of Size-Resolved Fluorescent Biological Aerosol Particles. *Indoor Air* **2015**, *26*, 193−206.
(83) Rosati, J. A.; Thornburg, J.; Rodes, C. Resuspension of Particulate Matter from Carpet Due to Human Activity. *Aerosol Sci. Technol.* **2008**, *42*, 472−482.
(84) Thio, B. J. R. *Characterization of Bioparticulate Adhesion to Synthetic Carpet Polymers with Atomic Force Microscopy*; Georgia Institute of Technology, 2008.
(85) Buttner, M. P.; Cruz-Perez, P.; Stetzenbach, L. D.; Garrett, P. J.; Luedtke, A. E. Measurement of Airborne Fungal Spore Dispersal from Three Types of Flooring Materials. *Aerobiologia* **2002**, *18*, 1−11.
(86) Booij-Noord, H.; De Vries, K.; Sluiter, H. J.; Orie, N. G. M. Late Bronchial Obstructive Reaction to Experimental Inhalation of House Dust Extract. *Clin. Exp. Allergy* **1972**, *2*, 43−61.
(87) Schuijs, M. J.; Willart, M. A.; Vergote, K.; Gras, D.; Deswarte, K.; Ege, M. J.; Madeira, F. B.; Beyaert, R.; van Loo, G.; Bracher, F.; von Mutius, E.; Chanez, P.; Lambrecht, B. N.; Hammad, H. Farm Dust and Endotoxin Protect against Allergy through A20 Induction in Lung Epithelial Cells. *Science* **2015**, *349*, 1106−1110.
(88) Booij-Noord, H.; Orie, N. G. M.; de Vries, K. Immediate and Late Bronchial Obstructive Reactions to Inhalation of House Dust and Protective Effects of Disodium Cromoglycate and Prednisolone. *J. Allergy Clin. Immunol.* **1971**, *48*, 344−354.
(89) Bornehag, C. G.; Nanberg, E. Phthalate Exposure and Asthma in Children. *Int. J. Androl.* **2010**, *33*, 333−345.
(90) Sercombe, J. K.; Liu-Brennan, D.; Causer, S. M.; Tovey, E. R. The Vertical Distribution of House Dust Mite Allergen in Carpet and the Effect of Dry Vacuum Cleaning. *Int. J. Hyg. Environ. Health* **2007**, *210*, 43−50.
(91) Causer, S. M.; Piper, C.; Shorter, C. L.; Lewis, R. D. Replicating the Cross-Sectional Distribution of House-Dust Mite Allergen Found in Carpet. *J. Text. Inst.* **2010**, *101*, 69−75.
(92) Shalat, S. L.; Stambler, A. A.; Wang, Z.; Mainelis, G.; Emoekpere, O. H.; Hernandez, M.; Lioy, P. J.; Black, K. Development and In-Home Testing of the Pretoddler Inhalable Particulate Environmental Robotic (PIPER Mk IV) Sampler. *Environ. Sci. Technol.* **2011**, *45*, 2945−2950.
(93) Shalat, S. L.; Lioy, P. J.; Schmeelck, K.; Mainelis, G. Improving Estimation of Indoor Exposure to Inhalable Particles for Children in the First Year of Life. *J. Air Waste Manage. Assoc.* **2007**, *57*, 934−939.
(94) Khare, P.; Marr, L. C. Simulation of Vertical Concentration Gradient of Influenza Viruses in Dust Resuspended by Walking. *Indoor Air* **2015**, *25*, 428−440.
(95) Hinds, W. C. *Aerosol Technology: Properties, Behavior, and Measurement of Airborne Particles*; John Wiley & Sons, 2012.
(96) Huffman, J. A.; Treutlein, B.; Pöschl, U. Fluorescent Biological Aerosol Particle Concentrations and Size Distributions Measured with an Ultraviolet Aerodynamic Particle Sizer (UV-APS) in Central Europe. *Atmos. Chem. Phys.* **2009**, *9*, 17705.
(97) Roberts, J. W.; Clifford, W. S.; Glass, G.; Hummer, P. G. Reducing Dust, Lead, Dust Mites, Bacteria, and Fungi in Carpets by Vacuuming. *Arch. Environ. Contam. Toxicol.* **1999**, *36* (4), 477−484.
(98) Layton, D. W.; Beamer, P. I. Migration of Contaminated Soil and Airborne Particulates to Indoor Dust. *Environ. Sci. Technol.* **2009**, *43*, 8199−8205.
(99) Jiang, Y.; Matsusaka, S.; Masuda, H.; Qian, Y. Characterizing the Effect of Substrate Surface Roughness on Particle−Wall Interaction with the Airflow Method. *Powder Technol.* **2008**, *186*, 199−205.
(100) Götzinger, M.; Peukert, W. Particle Adhesion Force Distributions on Rough Surfaces. *Langmuir* **2004**, *20*, 5298−5303.
(101) Goldasteh, I.; Ahmadi, G.; Ferro, A. A Model for Removal of Compact, Rough, Irregularly Shaped Particles from Surfaces in Turbulent Flows. *J. Adhes.* **2012**, *88*, 766−786.
(102) Soltani, M.; Ahmadi, G. Direct Numerical Simulation of Particle Entrainment in Turbulent Channel Flow. *Phys. Fluids* **1995**, *7*, 647−657.
(103) Ziskind, G.; Fichman, M.; Gutfinger, C. Resuspension of Particulates from Surfaces to Turbulent Flows—Review and Analysis. *J. Aerosol Sci.* **1995**, *26*, 613−644.
(104) Soltani, M.; Ahmadi, G. Detachment of Rough Particles with Electrostatic Attraction from Surfaces in Turbulent Flows. *J. Adhes. Sci. Technol.* **1999**, *13*, 325−355.
(105) Schaefer, D. M.; Carpenter, M.; Gady, B.; Reifenberger, R.; Demejo, L. P.; Rimai, D. S. Surface Roughness and Its Influence on Particle Adhesion Using Atomic Force Techniques. *J. Adhes. Sci. Technol.* **1995**, *9*, 1049−1062.
(106) Pakarinen, O. H.; Foster, A. S.; Paajanen, M.; Kalinainen, T.; Katainen, J.; Makkonen, I.; Lahtinen, J.; Nieminen, R. M. Towards an Accurate Description of the Capillary Force in Nanoparticle-Surface Interactions. *Modell. Simul. Mater. Sci. Eng.* **2005**, *13*, 1175.
(107) Jones, R.; Pollock, H. M.; Cleaver, J. A. S.; Hodges, C. S. Adhesion Forces between Glass and Silicon Surfaces in Air Studied by AFM: Effects of Relative Humidity, Particle Size, Roughness, and Surface Treatment. *Langmuir* **2002**, *18*, 8045−8055.
(108) Butt, H.-J.; Kappl, M. Normal Capillary Forces. *Adv. Colloid Interface Sci.* **2009**, *146*, 48−60.
(109) Hooton, J. C.; German, C. S.; Allen, S.; Davies, M. C.; Roberts, C. J.; Tendler, S. J. B.; Williams, P. M. An Atomic Force Microscopy Study of the Effect of Nanoscale Contact Geometry and Surface Chemistry on the Adhesion of Pharmaceutical Particles. *Pharm. Res.* **2004**, *21*, 953−961.
(110) Busnaina, A. A.; Elsawy, T. The Effect of Relative Humidity on Particle Adhesion and Removal. *J. Adhes.* **2000**, *74*, 391−409.
(111) Ferro, A. R.; Kopperud, R. J.; Hildemann, L. M. Source Strengths for Indoor Human Activities That Resuspend Particulate Matter. *Environ. Sci. Technol.* **2004**, *38*, 1759−1764.
(112) Lai, A. C. K.; Thatcher, T. L.; Nazaroff, W. W. Inhalation Transfer Factors for Air Pollution Health Risk Assessment. *J. Air Waste Manage. Assoc.* **2000**, *50*, 1688−1699.

https://dx.doi.org/10.1021/acs.est.0c06157
Environ. Sci. Technol. 2021, 55, 1864−1875

(113) Hernandez, M.; Perring, A. E.; McCabe, K.; Kok, G.; Granger, G.; Baumgardner, D. Chamber Catalogues of Optical and Fluorescent Signatures Distinguish Bioaerosol Classes. *Atmos. Meas. Tech.* **2016**, *9*, 3283−3292.
(114) Qian, J.; Hospodsky, D.; Yamamoto, N.; Nazaroff, W. W.; Peccia, J. Size-resolved Emission Rates of Airborne Bacteria and Fungi in an Occupied Classroom. *Indoor Air* **2012**, *22*, 339−351.
(115) Adolph, K. E. Motor and Physical Development: Locomotion. *Encyclopedia of Infant and Early Childhood Development*; Elsevier Inc., 2008; pp 359−373.

https://dx.doi.org/10.1021/acs.est.0c06157
Environ. Sci. Technol. 2021, 55, 1864−1875